# Modern Magnetic Resonance Imaging Modalities to Advance Neuroimaging in Astronauts

Lila Berger; Ford Burles; Tejdeep Jaswal; Rebecca Williams; Giuseppe Iaria

**INTRODUCTION:** The rapid development of the space industry requires a deeper understanding of spaceflight's impact on the brain. MRI research reports brain volume changes following spaceflight in astronauts, potentially affecting cognition. Recently, we have demonstrated that this evidence of volumetric changes, as measured by typical T1-weighted sequences (e.g., magnetization-prepared rapid gradient echo sequence; MPRAGE), is error-prone due to the microgravity-related redistribution of cerebrospinal fluid in the brain. More modern neuroimaging methods, particularly dual-echo MPRAGE (DEMPRAGE) and magnetization-prepared rapid gradient echo sequence utilizing two inversion pulses (MP2RAGE), have been suggested to be resilient to this error. Here, we tested if these imaging modalities offered consistent segmentation performance improvements in some commonly employed neuroimaging software packages.

**METHODS:** We conducted manual gray matter tissue segmentation in traditional T1w MRI images to utilize for comparison. Automated tissue segmentation was performed for traditional T1w imaging, as well as on DEMPRAGE and MP2RAGE images from the same subjects. Statistical analysis involved a comparison of total gray matter volumes for each modality, and the extent of tissue segmentation agreement was assessed using a test of similarity (Dice coefficient).

**RESULTS:** Neither DEMPRAGE nor MP2RAGE exhibited consistent segmentation performance across all toolboxes tested.

**DISCUSSION:** This research indicates that customized data collection and processing methods are necessary for reliable and valid structural MRI segmentation in astronauts, as current methods provide erroneous classification and hence inaccurate claims of neuroplastic brain changes in the astronaut population.

**KEYWORDS:** tissue segmentation, spaceflight, gray matter, dura, cerebrospinal fluid, volumetry.

**Berger L, Burles F, Jaswal T, Williams R, Iaria G. *Modern magnetic resonance imaging modalities to advance neuroimaging in astronauts*. Aerosp Med Hum Perform. 2024; 95(5):245–253.**

As the space industry progresses toward long-range space exploration,[1] it is becoming increasingly vital to understand the implications of space travel on the well-being of astronauts. This rapid growth can be attributed in part to the privatization of the industry, as companies have begun partnering with government agencies such as NASA to begin sending more civilians to space than ever before.[2] As of 2021, there have been over 600 astronauts that have been to space, and this number will only continue to increase as new plans develop to return to the moon.[3,4] Increases in the number of humans going to space presents both a necessity and an opportunity to study the effects of space travel on the brain.

Studies utilizing MRI have provided evidence that spaceflight causes structural changes to the brain.[5] These structural changes have the potential to impact the performance and safety of astronauts, therefore jeopardizing the success of space missions. For instance, Koppelmans and colleagues reported significant widespread decreases in gray matter (GM) volume postflight in the temporal and frontal lobes, precentral and postcentral gyrus, alongside various other changes in other brain regions.[6] These regions are necessary for various cognitive processes and for effective functioning, such as movement, planning, and decision-making.[7,8] Together, these studies suggest that exposure to microgravity (among other factors), as experienced during a spaceflight, has a significant effect on the

From the University of Calgary, Calgary, AB, Canada.

This manuscript was received for review in November 2023. It was accepted for publication in February 2024.

Address correspondence to: Mrs. Lila Berger, MSc, 2500 University Dr NW, Calgary, Alberta T2N 1N4, Canada; lb63@rice.edu.



DOI: https://doi.org/10.3357/AMHP.6395.2024

volumes of selective regions in the brain, which may have an impact on the performance of astronauts during space missions.[9]

In addition to GM and white matter (WM) volume changes, spaceflight has also been shown to lead to changes in the distribution of cerebrospinal fluid (CSF) within the skull as an effect of exposure and adaptation to microgravity.[6,9,10] Common cognitive repercussions attributed to CSF redistribution in the brain include worsening memory function and the occurrence of the spaceflight-associated neuro-ocular syndrome (SANS),[10,11] which is reported in approximately one third of astronauts and is correlated with increases in ventricular volume.[12] SANS affects the vision of astronauts, posing significant risks to the performance and safety of crewmembers.[9]

Importantly, in addition to CSF redistribution, exposure to microgravity has been reported to have an impact on the location of the entire brain within the skull,[13] resulting in an upward shifting of the brain and local alterations in the distribution of CSF.[14,15] We have recently investigated this issue in order to examine the potential effects of preprocessing procedures on the data analyses investigating the volumetric brain changes related to spaceflight.[15] We demonstrated that relocation of the brain within the skull results in GM tissue segmentation errors, with the dura (part of the meninges surrounding the brain) being the most commonly misclassified tissue.[15] Notably, tissue segmentation in this context refers to the process of dividing a neuroimage into segments that represent various tissue classes, such as GM, WM, and CSF.[16] Segmentation that is accurate and reliable is critical, as it can be used to diagnose tumors, inflammation, and lesions, as well as make general claims about neuroscience.[16] As such, errors in segmentation can lead to misdiagnoses, among other negative effects. We suggested that for the astronaut population, the misclassification of tissue may cause artifactual claims of volumetric brain changes during spaceflight, and it could explain the inconsistency reported in the literature addressing the issue of volumetric brain changes resulting from space travel.[15]

To properly understand the neurological impact that spaceflight has on the brain, it is necessary to identify the proper imaging modalities to best capture these changes, while also avoiding this misclassification of tissues. Droby and colleagues have suggested using newer scans such as a version of a magnetization-prepared rapid gradient echo sequence utilizing two inversion pulses (MP2RAGE) to obtain greater contrast between tissue types and correct for bias, which has been suggested to outperform the traditional magnetization-prepared rapid gradient echo sequence (MPRAGE) in automated segmentation software.[17–19] Additionally, Viviani and colleagues have provided evidence that the use of a dual-echo MPRAGE can provide better contrast between tissues and therefore improve segmentation accuracy.[20] The DEMPRAGE modality was selected due to the literature support of its high spatial resolution as well as minimal distortion, as a result of its increased readout bandwidth. Research has reported its ability to provide superior GM/dura segmentation, which typically appear similar in commonly used T1-weighted scans,[21,22] and it has been demonstrated to produce more reliable volume estimates for cortical structures as well.[23] Specifically, these two modalities have been suggested to improve the contrast between the dura and the other tissues in the brain.[17,20] In the present study, a BRAin VOlume imaging scan (BRAVO) was chosen as the standard or comparison modality for this research, due to its popularity throughout the literature regarding its tissue contrast and spatial resolution.[24] We hypothesized that these newer modalities may reduce the propensity of artifactual segmentation in the brains of astronauts, therefore improving our knowledge regarding the true impacts of spaceflight on the brain.

## METHODS

### Subjects

We acquired 20 healthy subjects (age mean/SD = 25.83/5.09 yr, 10 men). Subjects were excluded from this research if they had unremovable metal in their body, were on dialysis, or if they had a history of kidney issues or other serious medical conditions that would put them at an increased risk. From each subject, we collected whole-head MRI data from three different scans acquired on a 3T General Electric Discovery 750 MR scanner at Foothills Medical Centre at the University of Calgary. Subjects signed written informed consent before MR images were acquired, and all features of study design were approved by the Calgary Conjoint Health Research Ethics Board at the University of Calgary (REB21-1942).

### Procedure

We acquired subject MRI data using a 3T General Electric Discovery 750 (DV26) MR scanner at the University of Calgary's Foothills Medical Centre. We collected three structural images for use in this study: a BRAin VOlume imaging scan (BRAVO; TR = 6.68 ms, TE = 2.94 ms, TI = 650 ms, FA = 10°, FOV 25.6 cm, 1 mm isotropic voxels, 3 min 44 s acquisition time), which was used as a manufacturer equivalent of the commonly used T1-weighted MPRAGE, a Dual-Echo Magnetization-Prepared RApid Gradient Echo sequence (DEMPRAGE; TR = 916 ms, $TE_1$ = 2.404 ms, $TE_2$ = 5.796 ms, TI = 900 ms, FA = 8°, FOV 25.6 cm, 1 mm isotropic voxels, 4 min 31 s acquisition time), as well as an MP2RAGE (TR = 7.176 ms, TE = 2.12 ms, $TI_1$ = 8 s, $FA_1$ = 7°, $TI_2$ = 2.2 s, $FA_2$ = 5°, FOV 25.6 cm, 1 mm isotropic voxels, 5 min 39 s acquisition time), a variation of the standard magnetization-prepared rapid gradient echo sequence which utilizes two inversion timepoints (**Figs. 1** and **2**).

Tissue segmentation was conducted in a region of interest (ROI) centered around the cerebellar tentorium (**Fig. 3**). The ROI "tentorium" encompasses the medial occipital cortex and cerebellar tentorium, spanning a rectangular prism from MNI −25, −99, −22 to MNI 25, −44, 18, as used by Burles and colleagues.[15] Then, we manually excluded the cerebellum from this ROI, resulting in the ROI depicted in Fig. 3. The cerebellar tentorium is a dural structure which separates the cerebellum from the cerebral hemispheres in the brain and supports the cerebrum from collapsing onto the cerebellum due to the effects of gravity (Fig. 3). On most T1 images of preflight astronauts as

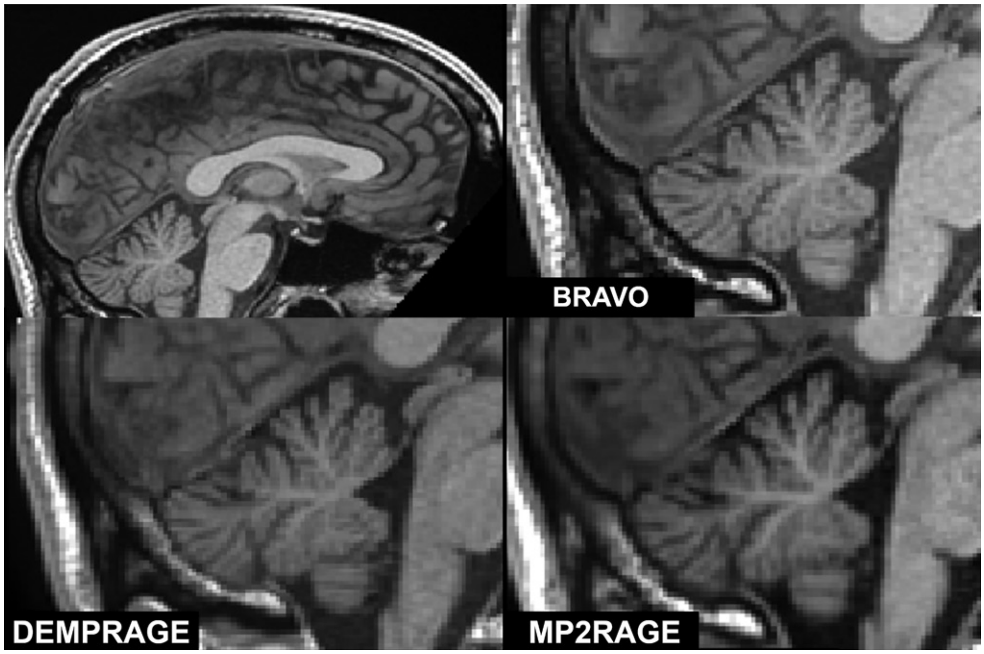


**Fig. 1.** MR images depict the various modalities collected. Top row depicts BRAVO, bottom left depicts DEMPRAGE, and the bottom right depicts MP2RAGE.

well as the typical research subject, the cerebellar tentorium is often misclassified as GM. The CSF shifts resulting from spaceflight[15] cause the tentorium and cerebral GM to spread apart, as typically the ventral portions of the cerebral cortex rest upon the tentorium. Due to this new space between the tissues, the dural tissue is less likely to be misclassified at postflight timepoints, therefore resulting in incorrect claims of GM losses in astronauts in nearby cortical regions due to spaceflight.[15] We utilized a tentorium ROI that did not include the cerebellum.

GM tissue segmentation was conducted manually by two tracers, L.B. and T.J., in the tentorium ROI. Here, we manually segmented the GM in the tentorium ROI in spaceflight-naive subjects, in which typical automated segmentation algorithms often misclassify large portions of the cerebellar tentorium as GM.[15] Manual GM segmentation was done using the commonly employed software ITK-SNAP[25] in the BRAVO modality of all subjects by both tracers. Manual segmentation of this region was performed to serve as the comparison with the automated segmentation,[26] as manual segmentation has been known throughout the literature as the segmentation method prone to the fewest large errors (i.e., systematic bias errors), although extremely labor intensive.[27]

After manual segmentation, we then utilized automated segmentation procedures from several software tools (Statistical

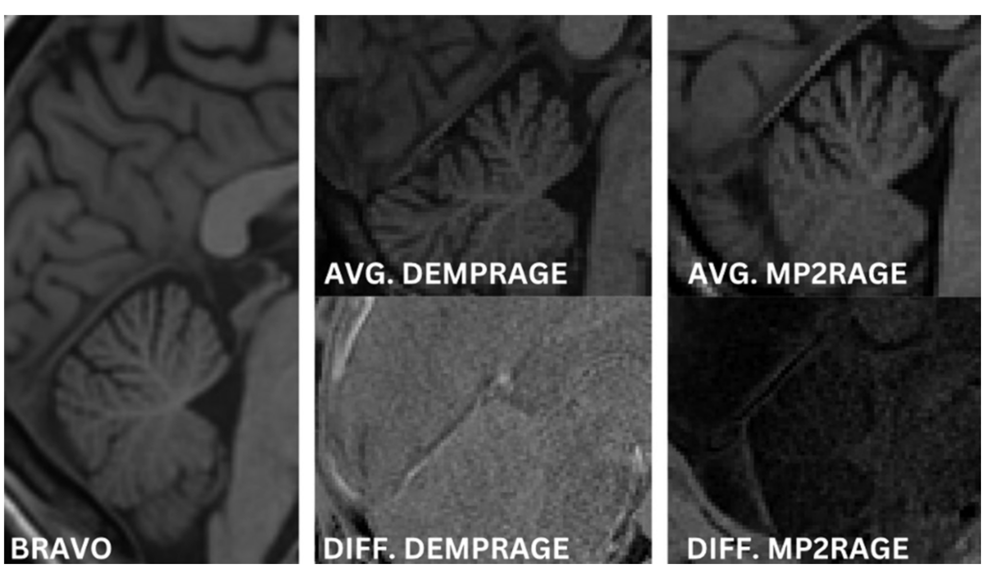


**Fig. 2.** MR images depict various modalities. The far-left image depicts the BRAVO modality, the top middle row depicts the average DEMPRAGE image combining both TEs, followed to the right by the average MP2RAGE image combining both TIs. The bottom middle row depicts the difference DEMPRAGE image, and the far-right image shows the MP2RAGE difference image. Note that the difference images clearly highlight the tentorium structure.

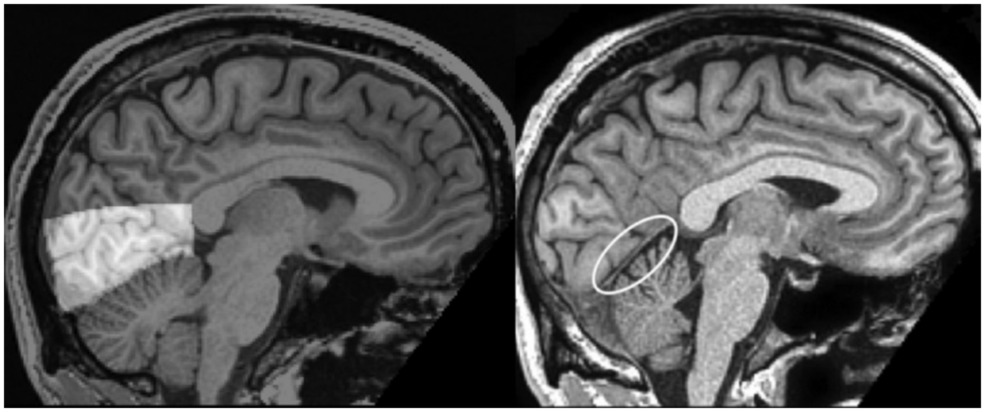

**Fig. 3.** Images depicting a native-space sample of the tentorium ROI used for tracing and segmentation (left) BRAVO. The right BRAVO image depicts the cerebellar tentorium.

Parametric Mapping 12 [SPM12], FSL 6.0.6, Freesurfer 7.2.0, and Advanced Normalization Tools [ANTs] 2.4.2) for comparison against manual segmentation. Generally, we utilized default or commonly reported settings with minimal adjustment to characterize naive performance of these algorithms with different imaging modalities.

SPM12 unified segmentation module[28] was used to independently segment all image modalities. Sampling distance was set to 1 mm, multiple volumes from the DEMPRAGE and MP2RAGE modalities were included as separate channels.

Images from all modalities were independently brain-extracted using the FSL brain-extraction tool (FSL-BET) with robust brain center estimation. The brain-extracted images were then segmented using FSL's automated segmentation tool (FSL-FAST) with default settings.[27]

Due to Freesurfer's limited capability to process multimodal or multivolume MR images as compared to other software packages, the DEMPRAGE and MP2RAGE four-dimensional images were each combined into three-dimensional volumes for processing. The images from the DEMPRAGE were combined by computing the root mean square value of each voxel across the volumes from each echo.[29] The images from the MP2RAGE modality were combined using the methodology provided by Knussman and colleagues, which multiplied the uniform image with the inversion ("second") image to remove background noise.[30] The unmodified BRAVO and these processed images were then segmented using Freesurfer's recon-all command, with no additional parameters. The cortical ribbon images output by recon-all were used as native-space GM segmentations for comparison with other methods. In contrast with the other automated segmentation procedures, the GM output selected from Freesurfer does not include GM from the cerebellum.

In the ANTs pipeline, the first step involved bias-field correcting images using N4BiasFieldCorrection;[31] each volume in the multivolume acquisitions was bias-field-corrected independently. We utilized the antsBrainExtraction.sh script with templates from the OASIS dataset[32] to generate brain masks for each imaging modality for each subject. These masks were then used to constrain segmentation using Atropos, performing a 3-tissue k-means classification.

Prior to analysis, GM probability maps from each MR modality from each segmentation software were binarized using a 0.5 threshold to classify all brain tissue as either GM (1) or nongray matter (0). This results in outputs that mimic the format of the manual segmentation and facilitates their comparison.

### Statistical Analysis

Dice coefficients were obtained for each subject across all modalities and automated segmentation software. Dice coefficients were also utilized to quantify the agreement between tracers (**Fig. 4**). The formula for the computation of Dice coefficients is:

$$Dice = \frac{2x|A \cap B|}{|A| + |B|}$$

Dice coefficients are the result of the spatial similarity of two segmentations, and this coefficient attempts to determine the amount of similarity between two (or more) sets of segmented regions or volumes; in the context of neuroimaging, the Dice coefficient is often used to quantify the accuracy of image

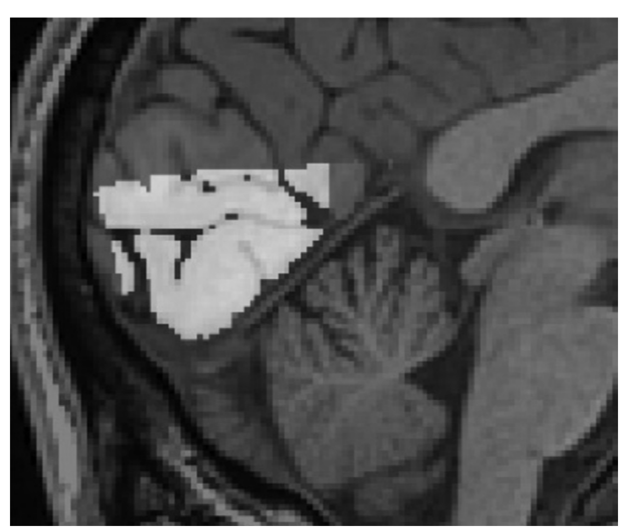

**Fig. 4.** White region indicative of overlap between manual tracers.

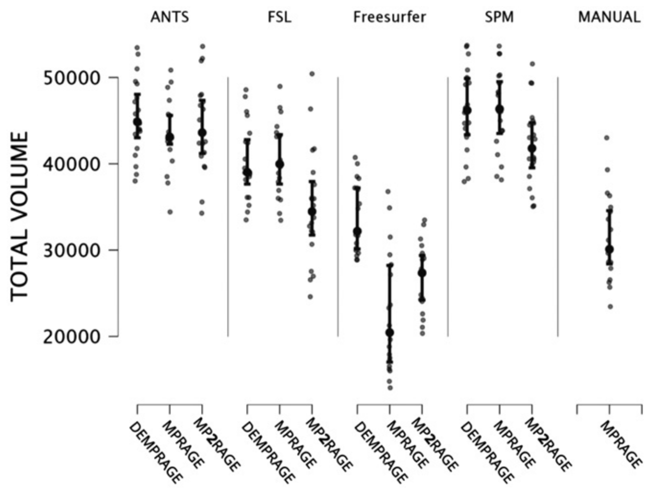


**Fig. 5.** Flexplot depicts total volume (voxels) estimates across the MPRAGE, MP2RAGE, and DEMPRAGE modalities across the ANTs, FSL, Freesurfer, and SPM12 software. Additionally, total volume estimates for the manual segmentation of the MPRAGE modality are also depicted. Voxels are in cubic millimeters.

segmentation algorithms, or between two or more tracers.[33] It can be calculated by taking the overlap between the two segmentations divided by the total number of pixels in both images and multiplying this by two, with higher Dice coefficients indicating greater agreement between the segmentations of two or more raters.[33] The total GM volume of the segmentation of the ROI was also obtained from all subjects in all modalities and software to determine the total number of voxels that were classified as GM to determine which automated segmentation software was the most liberal or conservative in their segmentation compared to the manual segmentation (**Fig. 5**). The manual segmentation of the MPRAGE modality reported an average total GM volume of 31,430 voxels (L.B. M = 30,558, SD = 5015 voxels; T.J. M = 32,301, SD = 5915 voxels). In order to compare interrater dice coefficients for all modalities against one another, we conducted two-tailed paired samples *t*-tests between each modality and software program. The significance threshold employed in this study was set at ≤0.05.

## RESULTS

Other studies utilizing Dice coefficients conclude that a Dice coefficient above 0.70 represents adequate agreement among individuals, and hence our tracing agreement (M = 0.84, SD = 0.03, MIN = 0.79, MAX = 0.89) is satisfactory and can represent our "ground truth" measure.[34] The average Dice coefficient between both tracers (**Fig. 6**) for the traditional MPRAGE scan was 0.84 (SD = 0.03). This average Dice coefficient suggests that both raters overlapped in their segmentation approximately 84% of all traced voxels. The MPRAGE modality was analyzed across segmentation software, and after statistical comparison with the manual segmentation, it was observed that the segmentation derived from SPM12 was the most similar to manual segmentation for the MPRAGE modality. SPM12 was followed by FSL,

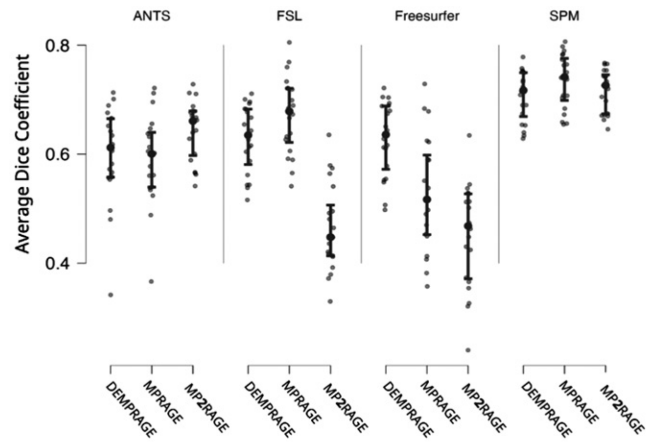


**Fig. 6.** Flexplot depicts the average dice coefficients for the MPRAGE, DEMPRAGE, and MP2RAGE modalities and between ANTs, FSL, Freesurfer, as well as SPM12 software.

ANTs, and then Freesurfer, which was the most unlike manual segmentation (**Table I**). The total ROI GM volume in MPRAGE was highest and therefore most liberal in SPM12, followed by ANTs, FSL, average manual segmentation, and finally Freesurfer with the most conservative GM classification (**Table II**).

The results of a paired samples *t*-test indicated that DEMPRAGE outperformed MP2RAGE when using FSL and Freesurfer, however the opposite was true when using SPM12 and ANTs (**Table III**). The DEMPRAGE modality Dice coefficients were analyzed next, and results indicated that they were significantly less similar to manual segmentation than the MPRAGE modality for SPM12 and FSL. However, DEMPRAGE significantly outperformed MPRAGE in Freesurfer, and nominally outperformed MPRAGE in ANTs as well (Table III). The total GM classification for DEMPRAGE was most liberal again in SPM12 and ANTs, followed by FSL and Freesurfer (Table II).

Finally, results indicated that MP2RAGE was less comparable to the manual segmentation in SPM12 and FSL, as well as Freesurfer. However, in ANTs, the MP2RAGE modality was shown to be more similar to manual segmentation than MPRAGE (Table I). Total volume calculations for the MP2RAGE modality were most liberal using ANTs, followed by SPM12, FSL, and Freesurfer (Table II).

**Table I.** Average Dice Coefficients Across Software.

| | MPRAGE | | DEMPRAGE | | MP2RAGE | |
|---|---|---|---|---|---|---|
| **SOFTWARE** | **M** | **SD** | **M** | **SD** | **M** | **SD** |
| SPM12 | 0.734 | 0.05 | 0.707 | 0.05 | 0.717 | 0.04 |
| FSL | 0.671 | 0.072 | 0.628 | 0.062 | 0.465 | 0.08 |
| Freesurfer | 0.528 | 0.105 | 0.628 | 0.069 | 0.452 | 0.097 |
| ANTS | 0.591 | 0.083 | 0.599 | 0.089 | 0.644 | 0.055 |
| Highest M Dice | SPM12 | | SPM12 | | SPM12 | |

Note: Depicts the average interrater Dice coefficients across modalities and automated segmentation software. The Dice coefficients from SPM12 were highest. The Dice coefficients from SPM12 and FSL were highest for the MPRAGE modality. In Freesurfer, the DEMPRAGE modality resulted in the highest Dice. In ANTs, MP2RAGE resulted in the highest Dice coefficient.

**Table II.** Total Volume.

| SOFTWARE | MPRAGE M | MPRAGE SD | DEMPRAGE M | DEMPRAGE SD | MP2RAGE M | MP2RAGE SD | HIGHEST M VOLUME |
|---|---|---|---|---|---|---|---|
| SPM12 | 46, 235 | 0.05 | 0.707 | 0.05 | 0.717 | 0.04 | DEMPRAGE |
| FSL | 40, 535 | 0.072 | 0.628 | 0.062 | 0.465 | 0.08 | MPRAGE |
| Freesurfer | 22, 660 | 0.105 | 0.628 | 0.069 | 0.452 | 0.097 | DEMPRAGE |
| ANTS | 43, 515 | 0.083 | 0.599 | 0.089 | 0.644 | 0.055 | DEMPRAGE |
| Manual Average | 31, 430 | 4910.3 | | | | | |
| Highest M Volume | SPM12 | | SPM12 | | ANTS | | |

Note: Total volume calculations between modalities and automated segmentation software. The total volume estimates from the MPRAGE and DEMPRAGE modalities were highest in SPM12.

## DISCUSSION

This study explored the use of DEMPRAGE and MP2RAGE modalities that were hypothesized to perform more similarly to a "ground truth" manual measure of segmentation,[18–20] resolving a newly established segmentation issue present among astronauts following a spaceflight mission.[15] To test this hypothesis, we compared the performance of automated software versus ground-truth manual segmentations for the three different image modalities. Contrary to our expectations, our results did not establish an obvious MR imaging modality that outperformed across all automated software. Instead, our findings suggest that the traditional MPRAGE modality still outperforms DEMPRAGE and MP2RAGE in terms of similarity to the manual segmentation in the automated software SPM12 and FSL. However, our results did indicate that DEMPRAGE and MP2RAGE perform most similarly to manual segmentation when using Freesurfer and ANTs, respectively. These findings are not surprising, as the literature reports challenges when selecting MR modality for automated segmentation, suggesting that no single methodological approach could be suitable for all images, not all methods could be conceived as equally effective for a particular type of image,[27] and there is no gold-standard software package to be adopted for brain segmentation.[17,35]

In order to determine which modality resulted in the most liberal and conservative GM classification among segmentation software, we analyzed their total volume estimates. Upon examining the results, a pattern emerged indicating that Freesurfer was extremely conservative in GM classification compared to all other segmentation software. One potential explanation for this bias is that although the cerebellum was removed in all ROIs, some cerebellar voxels may have possibly eluded this deletion. Freesurfer may have avoided segmentation of the cerebellum more accurately than others, resulting in less voxels being classified. Hence, it is a possibility that the Dice coefficients were also affected by this conservative bias in GM volume, as on average Freesurfer had significantly lower average Dice coefficients than other software in MPRAGE and MP2RAGE, and only 0.002 from the lowest Dice coefficient for DEMPRAGE. This finding seems to suggest that Freesurfer may have reported less GM on average than other software, or simply was most conservative in its GM classification, resulting in a lower similarity as less GM voxels were reported. Various literature echoes this concern, as some researchers report that Freesurfer underperforms in regard to robustness and consistency of automated segmentation in comparison to other software.[36,37]

Another possible explanation for our results indicating that these newer modalities only perform better in certain software may be that the automated segmentation software we selected had not been developed with the purpose of segmenting these newer imaging modalities.[17] These software were, presumably, developed specifically to segment BRAVO/MPRAGE MR images.[38] Hence, it is possible that the default segmentation parameters used in traditional MPRAGE modality are not optimized for the newer scans and may consequently impact segmentation performance.[15]

This concept was further supported by visually inspecting the newer modalities (Figs. 1 & 2). In Figs. 1 and 2, it appears significantly easier to differentiate the tentorium from the surrounding GM in the newer DEMPRAGE and MP2RAGE modalities than in the traditional modality. This visual observation suggests that image sequence parameter optimization is possible and may improve the accuracy of these newer modalities. The images obtained using default parameters on the GE MRI scanner and could potentially be improved.

As previous research has suggested that general pipelines were sufficient or were vague in their methods of pipeline optimization,[10,20,39] we did not investigate pipeline optimization and utilized default settings for all modalities to provide a

**Table III.** Dice Coefficient Comparison.

| SOFTWARE | MPRAGE > DEMPRAGE *t* | df | *P* | MPRAGE > MP2RAGE *t* | df | *P* | DEMPRAGE > MP2RAGE *t* | df | *P* |
|---|---|---|---|---|---|---|---|---|---|
| SPM12 | 10.25 | 38 | <0.001*** | 4.12 | 38 | <0.001*** | −3.54 | 38 | 0.002** |
| FSL | 6.68 | 38 | <0.001*** | 12.75 | 38 | <0.001*** | 12.05 | 38 | <0.001*** |
| Freesurfer | −4.8 | 38 | <0.001*** | 2.93 | 38 | <0.001*** | 14.07 | 38 | <0.001*** |
| ANTS | −0.43 | 38 | 0.67 | −4.81 | 38 | <0.001*** | −2.76 | 38 | 0.013* |

Note: Interrater Dice coefficient *t*-tests among the MPRAGE, DEMPRAGE, and MP2RAGE modalities, and across the SPM12, FSL, Freesurfer, and ANTs modalities. * = $P < 0.05$; ** = $P < 0.01$; *** = $P < 0.001$.

baseline measure of segmentation accuracy. Future research could expand upon the default settings to better optimize segmentation performance in automated software. There are possible adjustments that could improve performance of automated segmentation using the newer DEMPRAGE and MP2RAGE modalities. SPM12 has the option of utilizing Diffeomorphic Anatomical Registration Through Exponentiated Lie Algebra (DARTEL) to improve normalization and segmentation precision, which has been demonstrated to be effective for segmentation research.[10,19,38] Another method to improve segmentation in SPM12 is to alter the number of Gaussians representing each tissue class and empirically determine which is best for each modality. This was recommended by Viviani and colleagues to fully realize the potential of multimodal segmentation, and it will be important to explore models of signal density in which the number of Gaussian components is varied to identify additional features of tissu.[20] In FSL, another potential optimization parameter involves the use of priors as dura is in a similar anatomical location irrespective of modality. Our research did not make use of priors in FSL as its default implementation does not use spatial priors. Finally, computing novel derivatives of raw images may also best capture the extra information DEMPRAGE and MP2RAGE provide, such as average and difference images (Fig. 2). Utilizing this extra information may also provide better segmentation results.

Our study was conceived with the intent of improving brain tissue segmentation accuracy in the astronaut population, however, non-astronaut data were utilized in this research. The primary reasoning for collecting data from non-astronaut subjects involved the challenging nature of sampling the astronaut population. Nonetheless, this factor does not theoretically impact the results or even the generalizability of this work, as the cerebellar tentorium region is error-prone in all individuals due to its proximity to surrounding GM tissue, regardless of occupation.

Another limitation of this work involved the analysis of only one ROI (i.e., the tentorium). Future work should analyze additional ROIs, including the cerebral falx. This dural structure has been, in fact, shown to be impacted by spaceflight specifically, so it would be a key ROI to investigate in data obtained in the astronaut population.[15] Since we have demonstrated in a previous study that spaceflight induces CSF shifts in the brain that cause the cerebral falx to crowd neighboring tissue and results in a similar GM/dura segmentation issue as reported here,[15] an in-depth analysis of the falx ROI may shed light on the impact of this CSF redistribution and tissue-crowding on automated segmentation accuracy. While the tentorium ROI used in this study provided a deeper understanding of the impact of CSF redistribution that results in increased space between dura and surrounding tissues, the falx ROI would indicate the effects of CSF shifts resulting in decreased space between tissue types, potentially reflecting different segmentation inaccuracies.

Another noteworthy limitation of the present study involves the limited MR modalities obtained and analyzed. DEMPRAGE and MP2RAGE were chosen based on previous support in the literature.[17,20] However, there are numerous other MR modalities that may improve the accuracy of automated segmentation performance. One example is the fast GM acquisition T1 inversion recovery (FGATIR), which has been shown to acquire images with higher resolution and sharper delineation of brain regions than T1 or T2 imaging.[40] The drawback of obtaining FGATIR images is the acquisition time, as it takes approximately twice the time to obtain compared to a MPRAGE acquisition time at 3 T.[40,41] Future work should investigate this modality among others that have the potential to resolve these issues possibly without the use of parameter optimization.

Finally, another prospective solution to this issue is to utilize a Gadolinium-based contrast agent (GBCA) during data collection. GBCAs accumulate in the meninges in the outer layer of the blood brain barrier, permitting easier segmentation from GM in T1-weighted images.[42] There is support in the literature for GBCAs in terms of contrast of blood vessels[43] and dura[44] among other tissues such as tumors. One major concession of GBCA use is that it poses a slight potential risk, as it must be filtered out of the body through the kidneys. Hence, certain populations would be ineligible for this contrast such as those undergoing dialysis, as they rarely have been shown to cause kidney damage.[45] Due to this complication, it is unlikely that GBCAs will present the universal solution to this segmentation problem.

Space exploration is a flourishing industry, with more humans going into space than ever before. In accordance with this rapid development and expansion, there is an increased obligation to better understand the impact space travel has on the brain. This work contributes to providing recommendations for those investigating this impact through the analysis of two newer MR modalities among manual tissue segmentation. However, the astronaut population is not the sole population that could benefit from this research since other neurological issues, such as traumatic brain injuries (TBIs), result in CSF changes in the brain.[46] This population is more appreciable, as approximately 1.5 million Americans are diagnosed with a TBI every year.[47] MRI is a commonly utilized diagnostic tool for neurological conditions such as TBIs, and hence the implications of this research are critical due to their prevalence. The accuracy of MRI segmentations is significant, as they aid in a clearer understanding of the neurological effects of such a common brain injury.

Patients receiving dialysis treatment are another potential population that could benefit from this research, as CSF volumetric decreases are reported in those undergoing dialysis.[48] This symptom causes similar crowding issues as spaceflight on the cerebral falx, as the space between certain regions decreases, causing segmentation to become increasingly difficult.[15] If individuals receiving dialysis were to sustain a neurological injury, it is very possible that the MRI segmentation would be erroneous. Hence, the research reported in this manuscript has important implications for many individuals and is not limited exclusively to astronauts.

The primary objective of this research was to pinpoint the MR modalities required to understand and solve the segmentation issues present among astronauts. Our findings revealed that advanced MR modalities could be collected to address this issue. However, this could not be the ultimate solution for the segmentation issues detected in the astronaut population, as the scans investigated in our study only improve segmentation in certain automated software. Further investigation needs to be done to determine whether specific parameters or alternative MR modalities could enhance segmentation precision across all major automated software, which would provide a better methodological approach to advance our understanding of the impact of space travel on the human brain.

## ACKNOWLEDGEMENTS

*Financial Disclosure Statement:* The authors have no competing interests to declare.

*Authors and Affiliations:* Lila Berger, MSc., Ford Burles, Ph.D., Tejdeep Jaswal, BSc., and Giuseppe Iaria, Ph.D., NeuroLab, Canadian Space Health Research Network, Department of Psychology, Hotchkiss Brain Institute, Alberta Children's Hospital Research Institute, University of Calgary, Calgary, AB, Canada; and Rebecca Williams, Ph.D., Faculty of Health, School of Human Services, Charles Darwin University, Darwin, NT, Australia.

## REFERENCES

1. Smith M, Craig D, Herrmann N, Mahoney E, Krezel J, et al. The Artemis program: an overview of NASA's activities to return humans to the Moon. 2020 IEEE Aerospace Conference; March 7–14, 2020; Yellowstone Conference Center, Big Sky, MT. New York City (NY): IEEE; 2020; 1–10.
2. Davenport C. NASA looks to private sector for successor to the International Space Station. Wilson Center. 2022 [Accessed January 23, 2023]. Available from https://www.wilsoncenter.org/article/nasa-looks-private-sector-successor-international-space-station.
3. Roulette J. 600 people have been to space after NASA Crew-3 launch. The New York Times. 2021 [Accessed April 26, 2023]. Available from: https://www.nytimes.com/2021/11/10/science/600-astronauts-space.html.
4. O'Shea C. NASA names astronauts to next Moon mission, first crew under Artemis. NASA. 2023 [Accessed April 26, 2023]. Available from: http://www.nasa.gov/press-release/nasa-names-astronauts-to-next-moon-mission-first-crew-under-artemis.
5. Roy-O'Reilly M, Mulavara A, Williams T. A review of alterations to the brain during spaceflight and the potential relevance to crew in long-duration space exploration. npj Microgravity. 2021; 7(5):1–9.
6. Koppelmans V, Bloomberg JJ, Mulavara AP, Seidler RD. Brain structural plasticity with spaceflight. npj Microgravity. 2016; 2:2.
7. El-Baba RM, Schury MP. Neuroanatomy, frontal cortex. In: StatPearls. Treasure Island (FL): StatPearls Publishing; 2022. Available from http://www.ncbi.nlm.nih.gov/books/NBK554483/.
8. Patel A, Biso GMNR, Fowler JB. Neuroanatomy, temporal lobe. Treasure Island (FL): StatPearls Publishing; 2022. Available from http://www.ncbi.nlm.nih.gov/books/NBK519512/.
9. Lee JK, Koppelmans V, Riascos RF, Hasan KM, Pasternak O, et al. Spaceflight-associated brain white matter microstructural changes and intracranial fluid redistribution. JAMA Neurol. 2019; 76(4):412–419.
10. Hupfeld KE, McGregor HR, Lee JK, Beltran NE, Kofman IS, et al. The impact of 6 and 12 months in space on human brain structure and intracranial fluid shifts. Cereb Cortex Commun. 2020; 1(1):tgaa023.
11. Carmichael OT, Kuller LH, Lopez OL, Thompson PM, Dutton RA, et al. Cerebral ventricular changes associated with transitions between normal cognitive function, mild cognitive impairment, and dementia. Alzheimer Dis Assoc Disord. 2007(1):14–24.
12. Barisano G, Sepehrband F, Collins HR, Jillings S, Jeurissen B, et al. The effect of prolonged spaceflight on cerebrospinal fluid and perivascular spaces of astronauts and cosmonauts. PNAS. 2022; 119(17):e2120439119.
13. Roberts DR, Albrecht MH, Collins HR, Asemani D, Chatterjee AR, et al. Effects of spaceflight on astronaut brain structure as indicated on MRI. N Engl J Med. 2017; 377(18):1746–1753.
14. Van Ombergen A, Jillings S, Jeurissen B, Tomilovskaya E, Rühl RM, et al. Brain tissue–volume changes in cosmonauts. N Engl J Med. 2018; 379(17): 1678–1680.
15. Burles F, Williams R, Berger L, Pike GB, Lebel C, Iaria G. The unresolved methodological challenge of detecting neuroplastic changes in astronauts. Life. 2023; 13(2):500.
16. Schick F. Tissue segmentation: a crucial tool for quantitative MRI and visualization of anatomical structures. MAGMA. 2016; 29(2):89–93.
17. Droby A, Thaler A, Giladi N, Hutchison RM, Mirelman A, et al. Whole brain and deep gray matter structure segmentation: quantitative comparison between MPRAGE and MP2RAGE sequences. PLoS ONE. 2021; 16(8):e0254597.
18. Mueller SG. Mapping internal brainstem structures using MP2RAGE derived T1 weighted and T1 relaxation images at 3 and 7 T. Hum Brain Mapp. 2020; 41(8):2173–2186.
19. Marques JP, Kober T, Krueger G, van der Zwaag W, Van de Moortele PF, Gruetter R. MP2RAGE, a self bias-field corrected sequence for improved segmentation and T1-mapping at high field. Neuroimage. 2010; 49(2): 1271–1281.
20. Viviani R, Pracht ED, Brenner D, Beschoner P, Stingl JC, Stöcker T. Multimodal MEMPRAGE, FLAIR, and R2* segmentation to resolve dura and vessels from cortical gray matter. Front Neurosci. 2017; 11:258.
21. van der Kouwe AJW, Benner T, Salat DH, Fischl B. Brain morphometry with multiecho MPRAGE. Neuroimage. 2008; 40(2):559–569.
22. Viviani R, Stöcker T, Stingl JC. Multimodal FLAIR/MPRAGE segmentation of cerebral cortex and cortical myelin. Neuroimage. 2017; 152: 130–141.
23. Yan S, Qian T, Maréchal B, Kober T, Zhang X, et al. Test-retest variability of brain morphometry analysis: an investigation of sequence and coil effects. Ann Transl Med. 2020; 8(1):12.
24. Nair G, Absinta M, Reich DS. Optimized T1-MPRAGE sequence for better visualization of spinal cord multiple sclerosis lesions at 3T. AJNR Am J Neuroradiol. 2013; 34(11):2215–2222.
25. Yushkevich PA, Gao Y, Gerig G. ITK-SNAP: an interactive tool for semi-automatic segmentation of multi-modality biomedical images. 2016 38th Annual International Conference of the IEEE Engineering in Medicine and Biology Society; August 16–20, 2016; Disney's Contemporary Resort at Walt Disney World® Resort, Lake Buena Vista, FL. New York City (NY): IEEE; 2016; 3342–3345.
26. Pardoe HR, Pell GS, Abbott DF, Jackson GD. Hippocampal volume assessment in temporal lobe epilepsy: how good is automated segmentation? Epilepsia. 2009; 50(12):2586–2592.
27. Despotović I, Goossens B, Philips W. MRI segmentation of the human brain: challenges, methods, and applications. Comput Math Methods Med. 2015; 2015:450341.
28. Ashburner J, Friston KJ. Unified segmentation. Neuroimage. 2005; 26(3): 839–851.
29. Greve D. User Contributions/FAQ—FreeSurfer Wiki. 2019 [Accessed April 30, 2023]. Available from https://surfer.nmr.mgh.harvard.edu/fswiki/UserContributions/FAQ#Q.Isitrecommendedthatpeopleusememprage.3FHowaretheyanalyzed.3FJustsqrtsumsqroftheechoes.3FOristheresomethingmoreelaborate.3F.
30. Knussmann GN, Anderson JS, Prigge MBD, Dean DC, Lange N, et al. Test-retest reliability of FreeSurfer-derived volume, area and cortical thickness from MPRAGE and MP2RAGE brain MRI images. Neuroimage Rep. 2022; 2(2):100086.
31. Tustison NJ, Avants BB, Cook PA, Zheng Y, Egan A, et al. N4ITK: improved N3 bias correction. IEEE Trans Med Imaging. 2010; 29(6): 1310–1320.
32. Marcus DS, Wang TH, Parker J, Csernansky JG, Morris JC, Buckner RL. Open Access Series of Imaging Studies (OASIS): cross-sectional MRI data

in young, middle aged, nondemented, and demented older adults. J Cogn Neurosci. 2007; 19(9):1498–1507.
33. Zou KH, Warfield SK, Bharatha A, Tempany CMC, Kaus MR, et al. Statistical validation of image segmentation quality based on a spatial overlap index. Acad Radiol. 2004; 11(2):178–189.
34. Zijdenbos AP, Dawant BM, Margolin RA, Palmer AC. Morphometric analysis of white matter lesions in MR images: method and validation. IEEE Trans Med Imaging. 1994; 13(4):716–724.
35. Choi US, Kawaguchi H, Matsuoka Y, Kober T, Kida I. Brain tissue segmentation based on MP2RAGE multi-contrast images in 7 T MRI. PLoS One. 2019; 14(2):e0210803.
36. Palumbo L, Bosco P, Fantacci ME, Ferrari E, Oliva P, et al. Evaluation of the intra- and inter-method agreement of brain MRI segmentation software packages: a comparison between SPM12 and FreeSurfer v6.0. Phys Med. 2019; 64:261–272.
37. Guo C, Ferreira D, Fink K, Westman E, Granberg T. Repeatability and reproducibility of FreeSurfer, FSL-SIENAX and SPM brain volumetric measurements and the effect of lesion filling in multiple sclerosis. Eur Radiol. 2019; 29(3):1355–1364.
38. González-Villà S, Oliver A, Valverde S, Wang L, Zwiggelaar R, Lladó X. A review on brain structures segmentation in magnetic resonance imaging. Artif Intell Med. 2016; 73:45–69.
39. Johnson EB, Gregory S, Johnson HJ, Durr A, Leavitt BR, et al. Recommendations for the use of automated gray matter segmentation tools: evidence from Huntington's disease. Front Neurol. 2017; 8:519.
40. Sudhyadhom A, Haq IU, Foote KD, Okun MS, Bova FJ. A high resolution and high contrast MRI for differentiation of subcortical structures for DBS targeting: the Fast Gray Matter Acquisition T1 Inversion Recovery (FGATIR). Neuroimage. 2009; 47(Suppl. 2):T44–T52.
41. Shepherd TM, Ades-Aron B, Bruno M, Schambra HM, Hoch MJ. Direct in vivo MRI discrimination of brain stem nuclei and pathways. AJNR. 2020; 41(5):777–784.
42. Ibrahim MA, Hazhirkarzar B, Dublin AB. Gadolinium magnetic resonance imaging. In: StatPearls. Treasure Island (FL): StatPearls Publishing; 2022 [Accessed March 8, 2023]. Available from http://www.ncbi.nlm.nih.gov/books/NBK482487/.
43. Ferris N, Goergen S. Gadolinium contrast medium (MRI contrast agents). Inside Radiology. 2016 [Accessed March 8, 2023]. Available from: https://www.insideradiology.com.au/gadolinium-contrast-medium/.
44. Suzuki M, Takashima T, Kadoya M, Ueda F, Yamashima T, Yamashita J. Gadolinium-DTPA enhancement of dural structures on MRI after surgery. Neurochirurgia (Stuttg). 1992; 35(4):112–116.
45. Zagoria R. CT and MRI Contrast and Kidney Function. UCSF Radiology. 2015 [Accessed March 28, 2023]. Available from: https://radiology.ucsf.edu/blog/abdominal-imaging/ct-and-mri-contrast-and-kidney-function.
46. Jha RM, Kochanek PM, Simard JM. Pathophysiology and treatment of cerebral edema in traumatic brain injury. Neuropharmacology. 2019; 145:230–246.
47. Thurman DJ, Alverson C, Dunn KA, Guerrero J, Sniezek JE. Traumatic brain injury in the United States: a public health perspective. J Head Trauma Rehabil. 1999; 14(6):602–615.
48. Funder J, Wieth JO. Changes in cerebrospinal fluid composition following hemodialysis. Scand J Clin Lab Invest. 1967; 19(4):301–312.